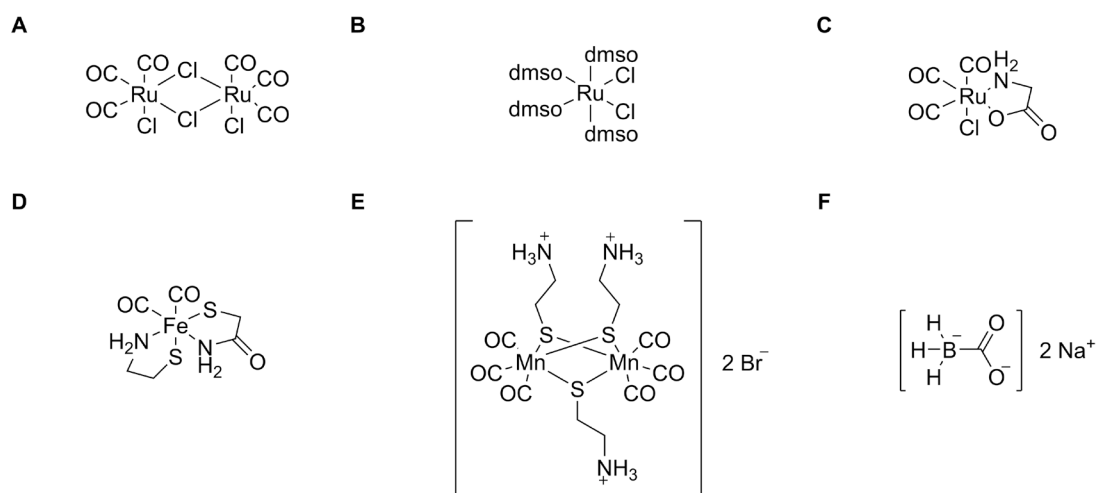


## CO-independent modification of K<sup>+</sup> channels by tricarbonyldichlororuthenium(II) dimer (CORM-2)

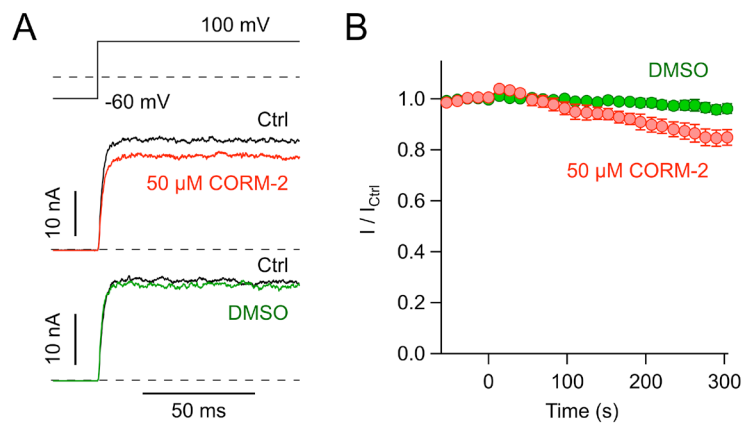
Guido Gessner<sup>a</sup>, Nirakar Sahoo<sup>a</sup>, Sandip M. Swain<sup>a</sup>, Gianna Hirth<sup>a</sup>, Roland Schönherr<sup>a</sup>, Ralf Mede<sup>b</sup>, Matthias Westerhausen<sup>b</sup>, Hans Henning Brewitz<sup>c</sup>, Pascal Heimer<sup>c</sup>, Diana Imhof<sup>c</sup>, Toshinori Hoshi<sup>d</sup>, and Stefan H. Heinemann<sup>a\*</sup>

### Supplementary Information

#### Supplementary Figures

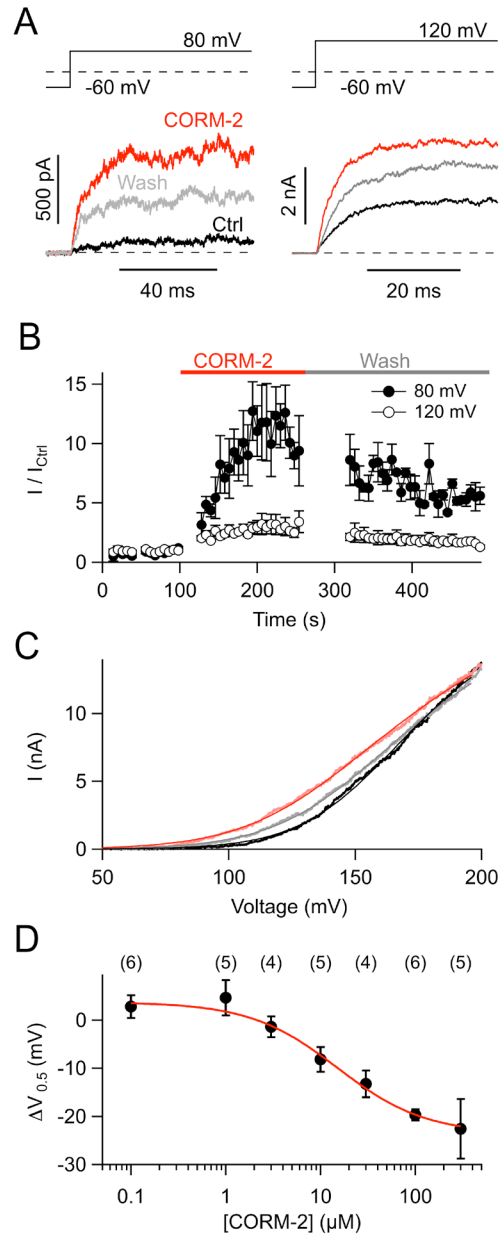


**Supplementary Fig. 1. Chemical structures of CORMs and putative degradation products used throughout this study.** A) CORM-2 (Tricarbonyldichlororuthenium(II) dimer), B) iCORM-2 (*Trans*-dichlorotetrakis(dimethylsulfoxide) ruthenium(II)), C) CORM-3 (Tricarbonylchloro(glycinato) ruthenium(II)), D) CORM-S1 (Dicarbonylbis(cysteamino) iron(II)), E) CORM-EDE1 ([Bis(tricarbonylmanganese)tris(cysteaminato)]) dihydrobromide, and F) CORM-A1 (Sodium boranocarbonate).

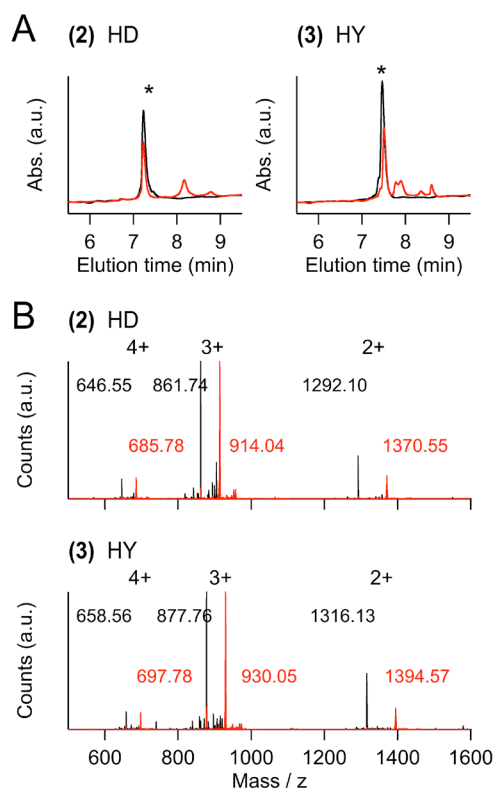


**Supplementary Fig. 2. External application of CORM-2 does not activate  $K_{Ca1.1}$  channels. A)**

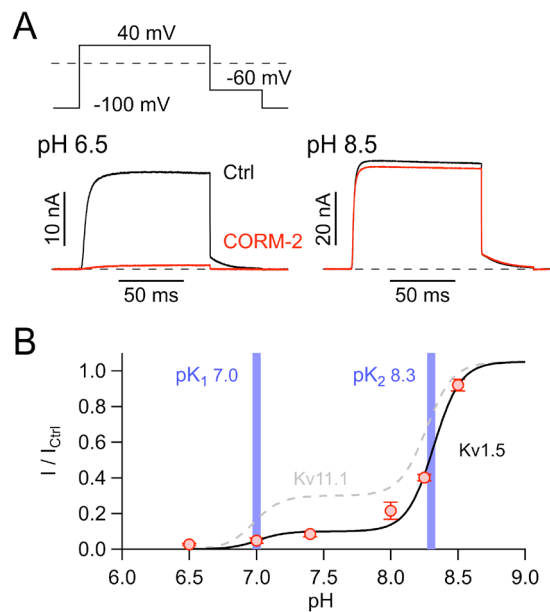
Representative  $K_{Ca1.1}$  whole-cell current traces for the indicated protocol before (Ctrl, black) and after application of 50  $\mu$ M CORM-2 (red) or vehicle (0.1% DMSO, green). The intracellular solution was free of  $Ca^{2+}$ . B) Normalized mean current at 100 mV as a function of time with CORM-2 and vehicle application at time = 0; means  $\pm$  S.E.M. for  $n = 5$ , each.



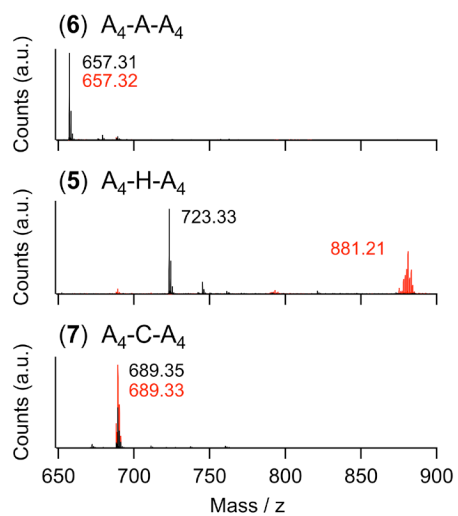
**Supplementary Fig. 3. Hallmarks of  $K_{Ca}1.1$  activation by CORM-2.** A) Representative  $K_{Ca}1.1$  current traces from inside-out patches before (Ctrl, black), in the presence (red), and after washout (grey) of 50  $\mu$ M CORM-2. B) Time course of mean current at 80 and 120 mV for CORM-2 application and washout. Means  $\pm$  S.E.M. for  $n = 3$ . C) Current responses to voltage ramps with superimposed fit according to:  $I(V) = (V - V_{rev}) * (G_{max} / (1 + \exp((V_{0.5} - V) / V_e)))$ , with the maximal conductance  $G_{max}$ , the half-activating voltage  $V_{0.5}$ , a slope factor  $V_e$  and the reversal potential  $V_{rev}$ . D) Change in  $V_{0.5}$  as a function of CORM-2 concentration with superimposed Hill fit yielding a maximal shift of  $V_{0.5}$  by -23.6 mV with an  $EC_{50}$  of 15.1  $\mu$ M and a Hill coefficient of 0.94. Data are means  $\pm$  S.E.M. with  $n$  indicated in parentheses. The intracellular solution was free of  $Ca^{2+}$ .



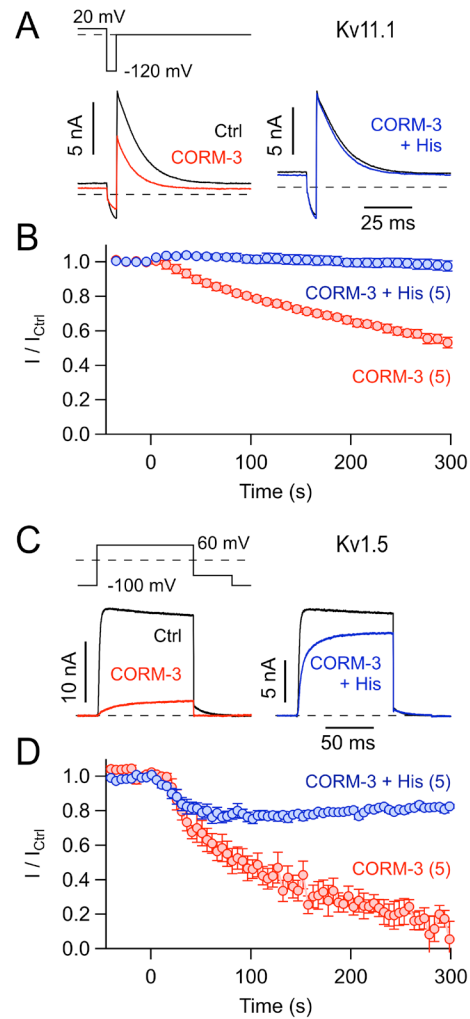
**Supplementary Fig. 4. Peptide modification by CORM-2.** A) HPLC elution profiles of 22-residue peptides corresponding to the pore loop sequences of mutant Kv11.1 channels (HD **(2)**, corresponding to H578D; HY **(3)**, corresponding to H587Y). Red traces are from peptides preincubated with CORM-2, black: peptides without preincubation. The elution peak for the non-modified peptides is marked with an asterisk. B) Mass spectra of wild-type and double-mutant peptides (as in (A)) before (black) and after incubation with CORM-2 (red). The labeled peaks correspond to  $(M+4H^+)^{4+}$ ,  $(M+3H^+)^{3+}$  and  $(M+2H^+)^{2+}$  of the peptides or the peptide:Ru(CO)<sub>2</sub> complexes.



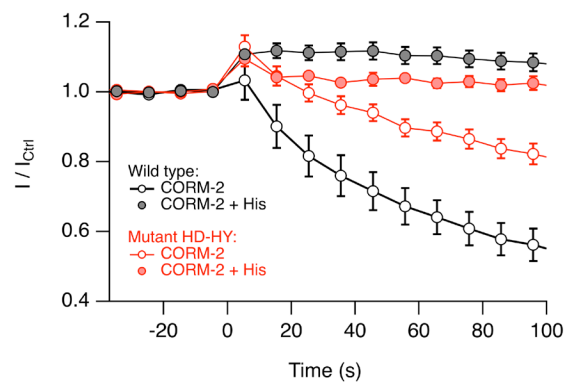
**Supplementary Fig. 5. pH dependence of Kv1.5 inhibition by CORM-2.** A) Representative traces of whole-cell Kv1.5 currents before (black) and 90 s after (red) application of 50  $\mu$ M CORM-2. B) Normalized mean remaining currents for various pH values fit with a two-component Hill function (solid line). Resulting pK values are indicated by vertical bars. Data in B are means  $\pm$  S.E.M. for  $n = 6-8$ . The dashed fit curve represents the result for Kv11.1 channels (cf. Fig. 6).



**Supplementary Fig. 6. Peptide modification by CORM-2.** Superimposed mass spectra of 9mer peptides (Ala (6), His (5) or Cys (7), flanked with 4 Ala on each side) before (black) and after 15-min incubation with 12.5  $\mu$ M CORM-2 (red). Mass increase equivalent to a Ru(CO)<sub>2</sub> adduct is detected in A<sub>4</sub>-H-A<sub>4</sub> only.

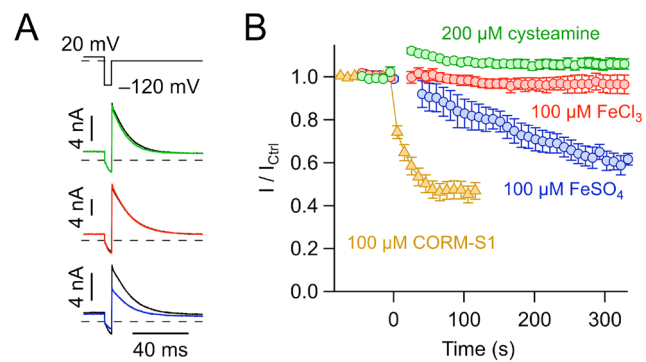


**Supplementary Fig. 7. Histidine-dependent current inhibition of Kv11.1 and Kv1.5 channels by CORM-3.** A) Pulse protocol and representative current traces of Kv11.1 channels before (black) and 5 min after application of 50  $\mu\text{M}$  CORM-3 without (red) or with 1  $\mu\text{M}$  histidine in the bath solution (blue). Depolarization to 20 mV lasted 400 ms (not shown). B) Time course of mean normalized currents with application of CORM-3 at time zero. C, D) As in A and B for Kv1.5 channels. Data as B and D are means  $\pm$  S.E.M. with  $n$  indicated in parentheses; straight lines connect the data points for clarity.



**Supplementary Fig. 8. Effect of CORM-2 on wild-type and mutant Kv11.1 channels.** Peak tail current of Kv11.1 channels with application of 50  $\mu$ M CORM-2 at time=0 for the wild type (black) and mutant H578D:H587Y (red) without (open) and with (filled circles) 1 mM free histidine in the bath. Data are means  $\pm$  S.E.M. with  $n = 5$  or 6.





**Supplementary Fig. 9. Effect of CORM-S1 breakdown products on Kv11.1 channels.** A) Pulse protocol and representative current traces of Kv11.1 channels before (black) and 5 min after application of 200 μM cysteamine (green), 100 μM FeCl<sub>3</sub> (red), or 100 μM FeSO<sub>4</sub> (blue). Depolarization to 20 mV lasted 400 ms (not shown). B) Time course of mean normalized currents with application of the indicated substances at time zero. Data are means ± S.E.M. with  $n = 5$  or 6.